Molecular Biology of the Cell
Vol. 10, 3891–3908, November 1999

Differential Roles of Syntaxin 7 and Syntaxin 8 in Endosomal Trafficking

Rytis Prekeris,*† Bin Yang,*† Viola Oorschot,‡ Judith Klumperman,‡ and Richard H. Scheller*§

*Howard Hughes Medical Institute, Department of Molecular and Cellular Physiology, Stanford University School of Medicine, Stanford, California 94305-5428; and ‡Medical School, University of Utrecht, Institute for Biomembranes, 3584CX Utrecht, The Netherlands

Submitted July 7, 1999; Accepted September 8, 1999
Monitoring Editor: Juan Bonifacino

To understand molecular mechanisms that regulate the intricate and dynamic organization of the endosomal compartment, it is important to establish the morphology, molecular composition, and functions of the different organelles involved in endosomal trafficking. Syntaxins and vesicle-associated membrane protein (VAMP) families, also known as soluble *N*-ethylmaleimide-sensitive factor (NSF) attachment protein receptors (SNAREs), have been implicated in mediating membrane fusion and may play a role in determining the specificity of vesicular trafficking. Although several SNAREs, including VAMP3/cellubrevin, VAMP8/endobrevin, syntaxin 13, and syntaxin 7, have been localized to the endosomal membranes, their precise localization, biochemical interactions, and function remain unclear. Furthermore, little is known about SNAREs involved in lysosomal trafficking. So far, only one SNARE, VAMP7, has been localized to late endosomes (LEs), where it is proposed to mediate trafficking of epidermal growth factor receptor to LEs and lysosomes. Here we characterize the localization and function of two additional endosomal syntaxins, syntaxins 7 and 8, and propose that they mediate distinct steps of endosomal protein trafficking. Both syntaxins are found in SNARE complexes that are dissociated by α-soluble NSF attachment protein and NSF. Syntaxin 7 is mainly localized to vacuolar early endosomes (EEs) and may be involved in protein trafficking from the plasma membrane to the EE as well as in homotypic fusion of endocytic organelles. In contrast, syntaxin 8 is likely to function in clathrin-independent vesicular transport and membrane fusion events necessary for protein transport from EEs to LEs.

INTRODUCTION

Eukaryotic cells use membranes to compartmentalize biological functions and as a selective barrier to isolate the interior of the cell from the surrounding environment. As part of the mechanism for establishing and maintaining homeostasis, cells sample the outside world through continuous endocytosis of the plasma membrane (PM). Cells face the challenge of sorting and transporting endocytosed molecules to the appropriate organelles. For example, ligands of surface receptors are often transported to lysosomes for degradation, whereas complex arrays of PM proteins are recycled back to the cell surface. Membrane trafficking decisions and the sorting of endocytosed proteins take place, at least in part, within early endosomes (EEs), also known as sorting endosomes (Helenius *et al.*, 1983; Mayor *et al.*, 1993). EEs comprise endosomal vacuoles that are continuous with a highly dynamic tubulovesicular network (Mellman, 1996). From the EE most membrane proteins are rapidly recycled back to the PM, whereas soluble proteins preferentially stay in the lumen and proceed toward the lysosome. The recycling of proteins from EEs involves generation and scission of the long tubular extensions. These tubules are also known as recycling endosomes (REs), because they lack late endosomal and lysosomal markers and are enriched in recycling

† These authors contributed equally to this work.

§ Corresponding author. E-mail address: scheller@cmgm.stanford.edu.

Abbreviations used: AP, adaptor protein; ATPγS, adenosine 5′-*O*-(thiotriphosphate); BFA, brefeldin A; CHO, Chinese hamster ovary; DMEM, Dulbecco's modified Eagle's medium; EE, early endosome; EGF, epidermal growth factor; EGFR, EGF receptor; ER, endoplasmic reticulum; GFP, green fluorescent protein; Ig, immunoglobulin; LE, late endosome; NRK, normal rat kidney; NSF, *N*-ethylmaleimide-sensitive factor; PM, plasma membrane; PNS, postnuclear supernatant; RE, recycling endosome; SNAP, soluble NSF attachement protein; SLO, streptolysin O; SNAP-25, synaptosomal-associated protein of 25 kDa; SNARE, soluble NSF attachement protein receptor; Tf, transferrin; TfR, transferrin receptor; TGN, *trans*-Golgi network; TxR, Texas Red; VAMP, vesicle-associated membrane protein.

membrane proteins (Hopkins, 1983; Hopkins and Trowbridge, 1983; Gruenberg and Maxfield, 1995).

A primary sorting mechanism in EEs seems to be, at least in part, due to the differences in surface-to-volume ratio in the distinct subcompartments, resulting in retention of the soluble contents in endosomal vacuoles and accumulation of membrane proteins in tubular extensions (Mellman, 1996). For instance, the return of fluorescent sphingolipid analogues to the PM occurs with kinetics indistinguishable from the kinetics of transferrin receptor (TfR) recycling (Mayor *et al.*, 1993). Moreover, the rapid recycling of mutant TfR lacking a cytosolic domain (Marsh *et al.*, 1995) suggests that membrane proteins follow the recycling pathway defined by membrane lipids in a signal-independent manner. However, the existence of additional clathrin-dependent sorting pathways that mediate the PM recycling of membrane proteins cannot be excluded.

The transport of proteins from EEs to lysosomes remains poorly understood. One model suggests that endosomal carrier vesicles bud from EEs and deliver a subset of proteins to late endosomes (LEs) or lysosomes (Gruenberg *et al.*, 1989). An alternative model suggests that EEs mature into LEs by losing EE characteristics, such as recycling proteins like TfR, but at the same time acquire characteristics of lysosomes, such as the presence of active acid hydrolases (Stoorvogel *et al.*, 1991; Futter *et al.*, 1996). A further complication in understanding lysosomal transport is the difficulty of defining the lysosomal compartment. Indeed, although it is clear that lysosomes have a distinct protein composition, many lysosomal proteins are delivered from the endosomes and can therefore be found in EEs, LEs, as well as mature lysosomes (Kornfield and Mellman, 1989).

Understanding the intricate and dynamic organization of the endosomal compartment is based on the ability to establish relationships among the morphological, biochemical, and functional definitions of the different organelles involved in endosomal trafficking. In recent years a set of proteins has emerged whose role is to mediate and regulate membrane fusion events. Syntaxins and vesicle-associated membrane protein (VAMP/synaptobrevin) families, also known as soluble *N*-ethylmaleimide-sensitive factor attachment protein receptors (SNAREs), have been implicated in mediating membrane fusion and may play a role in determining specificity of vesicular trafficking (Bennett *et al.*, 1993; Bennett and Scheller, 1993; Sollner *et al.*, 1993b). Membrane fusion has been proposed to be mediated by the formation of very stable core complexes, comprising four α-helices. In the ternary synaptic complex, the PM syntaxin (qSNARE) contributes one α-helix, centered on a glutamate residue, whereas the vesicle protein VAMP (rSNARE) provides another helical domain, centered on an arginine residue (Sutton *et al.*, 1998). The remaining two helices are contributed by the PM synaptosomal-associated protein of 25 kDa (SNAP-25) and are also centered on glutamate residues (Sutton *et al.*, 1998). A key feature of the SNARE hypothesis is that a qSNARE interacts with an appropriate rSNARE to form an organelle-specific docking complex, which ensures that transport vesicles fuse only with appropriate acceptor membranes (Sollner *et al.*, 1993b). Although recent evidence in vitro has questioned the ability of rSNARE–qSNARE interactions to determine membrane fusion specificity (Fasshauer *et al.*, 1999; Yang *et al.*, 1999), it has become apparent that specific SNAREs localize to distinct subcellular compartments, suggesting that SNARE interactions with other modulatory proteins may in fact regulate organelle transport and fusion.

Several SNAREs, including VAMP3/cellubrevin, VAMP8/endobrevin, syntaxin 13, and syntaxin 7, have been localized to the endosomal membranes (McMahon *et al.*, 1993; Advani *et al.*, 1998; Prekeris *et al.*, 1998; Wong *et al.*, 1998a,b). Syntaxin 13 is mainly found in REs and tubular extensions of EEs, where it mediates the PM recycling of TfR, presumably through binding to VAMP3/cellubrevin (Prekeris *et al.*, 1998). In agreement with this, previous studies have also demonstrated that VAMP3/cellubrevin is necessary for the efficient TfR trafficking to the PM (Galli *et al.*, 1994). However, the localization, biochemical interactions, and function of the other endosomal SNAREs remain unclear. Furthermore, little is known about SNAREs involved in lysosomal trafficking. So far, only one SNARE, VAMP7, has been localized to LEs, where it is proposed to mediate trafficking of epidermal growth factor receptor (EGFR) to LEs and lysosomes (Advani *et al.*, 1998, 1999).

If each distinct trafficking step requires a specific subset of VAMP and syntaxin proteins, many SNAREs would be expected to be involved in endosomal and lysosomal trafficking. Here we characterize the localization and function of two additional endosomal syntaxins that are involved in distinct steps of protein trafficking. Syntaxin 7 is mainly localized in vacuolar EEs and may be involved in protein trafficking from the PM to the EE. In contrast, syntaxin 8 is likely to function in vesicular transport and membrane fusion events necessary for protein transport from EEs to LEs.

MATERIALS AND METHODS

Materials and Antibodies

Cell culture reagents were obtained from Life Technologies (Gaithesburg, MD) unless otherwise specified. Texas Red (TxR)-labeled transferrin and FITC-labeled EGF were purchased from Molecular Probes (Eugene, OR). Enhanced chemiluminescence reagents were obtained from Amersham (Buckinghamshire, England). Human diferric ^{125}I-transferrin and ^{125}I-EGF were obtained from DuPont NEN (Wilmington, DE). Miscellaneous chemicals were obtained from Sigma (St. Louis, MO) and Fisher Biochemicals (Santa Clara, CA).

Anti-syntaxin 7 and anti-syntaxin 8 antibodies were prepared by immunization with bacterially expressed full-length cytoplasmic domain of syntaxin 7 and H3 domain of syntaxin 8 (aa 141–216). Polyclonal antibodies were then affinity purified from rabbit antisera as described previously (Bock *et al.*, 1997). Anti-VAMP 7 monoclonal and anti-syntaxin 13 polyclonal antibodies were described previously (Prekeris *et al.*, 1998; Advani *et al.*, 1999). Mouse anti-TfR antibodies were purchased from Zymed Laboratories (South San Francisco, CA). Mouse monoclonal anti-LAMP1 antibody was obtained from PharMingen (San Diego, CA). TxR- and Cy5-labeled anti-rabbit immunoglobulin G (IgG) and FITC-labeled anti-mouse IgG antibodies were obtained from Jackson Immuno Research (West Grove, PA). Mouse monoclonal anti-clathrin heavy chain antibody was obtained from Transduction laboratories (Lexington, KY).

Cell Culture and Immunofluorescence Microscopy

HeLa, Chinese hamster ovary (CHO), normal rat kidney (NRK), and NIH3T3 cells were grown in Dulbecco's modified Eagle's medium (DMEM) supplemented with 10% FCS, 100 U/ml penicillin, and 100 μg/ml streptomycin in humidified incubators with 5% CO_2 at 37°C.

Jurkat cells were grown in RPMI 1640 media containing 10% FCS, 100 U/ml penicilin, 100 μg/ml streptomycin, and 50 μM β-mercaptoethanol. Before each internalization experiment cells were incubated for 1 h in internalization media, consisting of DMEM with 50 mM HEPES, pH 7.4, and 3% BSA. Labeled transferrin or EGF was then added at a concentration of 60 or 1 μg/ml, respectively, and incubated as described in RESULTS. Cells were then chilled on ice, washed extensively with ice-cold PBS, and processed for immunofluorescence analysis. For pulse–chase experiments, after a PBS wash cells were overlaid with internalization media containing unlabeled transferrin or EGF and incubated at 37°C as described in RESULTS. Cells were then washed again with ice-cold PBS and processed for immunofluorescence or velocity centrifugation.

For immunofluorescence microscopy low-density NIH3T3, HeLa, Cos7, and NRK cells were fixed with 4% paraformaldehyde for 30 min. Cells were then permeabilized in 0.4% saponin, and nonspecific sites were blocked with PBS containing 0.2% BSA, 0.4% saponin, and 1% goat serum. Antisera were used at the following dilutions: anti-syntaxin 7 polyclonal antibody at 1 μg/ml; anti-syntaxin 8 polyclonal antibody at 1 μg/ml; anti-TfR monoclonal antibody at 1 μg/ml; and anti-syntaxin 6 monoclonal antibody at 2 μg/ml. FITC-labeled anti-mouse IgG and TxR-labeled anti-rabbit IgG were used at 7.5 μg/ml. After washes samples were mounted in Vecta-Shield (Vector Laboratories, Burlingame, CA). Immunofluorescence localization was performed on NRK, Cos7, NIH3T3, and HeLa cells using a Molecular Dynamics laser confocal imaging system (Beckman Center Imaging Facility, Stanford University).

Glycerol Velocity Gradients

Four 100-mm plates of either CHO or HeLa cells were homogenized in 20 mM HEPES, pH 7.4, containing 120 mM KCl, 2 mM EDTA, 2 mM EGTA, 1 mM DTT, 0.1 mM PMSF, 2 μg/ml leupeptin, 4 μg/ml aprotonin, and 0.8 μg/ml pepstatin, using a glass-Teflon homogenizer. Postnuclear supernatant (PNS) was obtained by centrifuging the homogenate at 2000 × *g* for 10 min twice. PNS was then extracted with 1% Triton X-100, and insoluble material was sedimented at 100,000 × *g* for 1 h. Glycerol gradients were prepared as described previously (Prekeris *et al.*, 1998). Samples were either control membrane extracts (see above) or extracts preincubated for 30 min with 250 μg/ml histidine-tagged *N*-ethylmaleimide-sensitive factor (NSF) and histidine-tagged α-soluble *N*-ethylmaleimide-sensitive factor attachement protein (α-SNAP), and either 500 μM adenosine 5′-*O*-(thiotriphosphate) (ATPγS) or 500 μM ATP with 8 mM $MgCl_2$.

Uptake of Anti-Green Fluorescent Protein (GFP) Antibodies

NRK cells were transiently transfected with syntaxin 7-GFP, syntaxin 13-GFP, or rbet1-GFP fusion proteins. Twenty-four hours after transfection cells were incubated with DMEM containing 10% FBS, 10 μg/ml cyclohexamide, and 5 μg/ml polyclonal rabbit anti-GFP antibody for varying amounts of time. Cells were then washed and chased for 15 min with DMEM containing 10% FBS. To determine the efficiency of anti-GFP uptake, cells were fixed and stained with anti-rabbit IgG conjugated to TxR and then imaged using confocal microscopy. To normalize for variations in fusion protein expression, the fluorescence intensity from the TxR fluoropore was divided by the fluorescence intensity of GFP. To measure the rate of antibody binding, cells were fixed, permeabilized with 0.4% saponin, and incubated for varying amounts of time with anti-GFP antibody before imaging with confocal microscopy.

In Vitro Trafficking of Tf and EGF in Streptolysin O (SLO)-permeabilized Cells

To measure EGF and Tf trafficking, we adopted with slight modifications the SLO-permeabilized cell system (Prekeris *et al.*, 1998). Briefly, HeLa cells were loaded with either I^{125}-EGF or I^{125}-Tf at 18°C for 1 h and then extensively washed to remove unbound EGF or Tf. Cells were then washed with KOAc(−) buffer (115 mM KOAc, 2.5 mM $Mg(OAc)_2$, and 25 mM HEPES, pH 7.4) containing 1 mM DTT and 1% BSA, followed by incubation on ice for 10 min with KOAc(−) buffer containing 15 μg/ml SLO (purchased from Dr. Sucharit Bhakdi, Johannes Gutenberg University, Mainz, Germany). The excess SLO was then removed by washing three times with KTM buffer [115 mM KoAc, 25 mM HEPES, pH 7.4, 2.5 mM $Mg(KoAc)_2$, and 1 mg/ml BSA]. To initiate permeabilization, cells were incubated at 18°C for 30 min, followed by incubation on ice for another 30 min, and extensively washed with KTM buffer. Under these conditions almost 95% of cytosol is removed from permeabilized cells (Prekeris *et al.*, 1998). Permeabilized cells were then resuspended in 0.5 ml of KTM buffer with or without 3 mg/ml rat brain cytosol. In all cases KTM buffer was supplemented with 0.5 mM ATP and an ATP regeneration system (80 mM creatine phosphate and 9 U/ml creatine kinase). EGF and Tf trafficking was induced by incubating samples at 37°C for 3 h. Under these conditions, EGF trafficking was restored to levels comparable with intact HeLa cells (Advani *et al.*, 1999). Where indicated, permeabilized HeLa cells were preincubated for 1 h with control IgG or anti-syntaxin 6, 7, or 8 antibodies. After incubation at 37°C, KTM buffer was removed, and cells were solubilized with 0.5 ml of KTM buffer containing 2% Triton X-100 to determine the EGF or Tf remaining in the cell. The Triton X-100 extracts represent released EGF and Tf. To determine the amount of degraded EGF, the removed buffer was extracted with 10% trichloroacetic acid. The precipitate containing recycled intact EGF (Renfrew and Hubbard, 1991; Futter *et al.*, 1996) was sedimented by centrifugation at 10,000 × *g* for 15 min. Remaining soluble I^{125} represents degraded EGF (Renfrew and Hubbard, 1991; Futter *et al.*, 1996). Unpublished data in our laboratory showed that similar trichloroacetic acid extraction of the buffer containing released I^{125}-Tf resulted in complete sedimentation of all I^{125}, in agreement with the data that Tf does not get targeted to the lysosomes for degradation. The amounts of degraded ^{125}I-EGF and recycled ^{125}I-Tf were determined by scintillation counting and expressed as percentage of total EGF or Tf (the sum of released and intracellular Tf or EGF for each sample).

The rat brain cytosol for EGF degradation and Tf recycling assays was prepared as described previously (Prekeris *et al.*, 1998). Briefly, fresh rat brains were homogenized in 25 mM HEPES, pH 7.4, containing 115 mM potassium acetate, 2.5 mM Mg-acetate, 0.1 mM EGTA, 2 mM DTT, 4 μg/ml aprotonin, and 0.8 μg/ml pepstatin. This homogenate was then subjected to centrifugation at 10,000 × *g* for 20 min, followed by centrifugating at 100,000 × *g* for 45 min. Cytosol was then flash frozen in liquid nitrogen and stored at −80°C. The protein concentration was determined by the Bradford assay according to the manufacturer's instructions (Bio-Rad, Hercules, CA).

Immunogold Labeling of Ultrathin Cryosections

CHO, PC12, and Cos7 cells were prepared for ultrathin cryosections and immunogold labeling as described previously (Slot *et al.*, 1991). In short, cells were fixed in 2% paraformaldehyde and 0.2% glutaraldehyde in 0.1 M phosphate buffer for 2 h at room temperature and postfixed overnight at 4°C in 2% paraformaldehyde. Then cells were washed with 0.02 M glycine in PBS, scraped off the dish, and pelleted in 10% gelatin in PBS, which was solidified on ice and cut into small blocks. After overnight infiltration with 2.3 M sucrose at 4°C for cryoprotection, blocks were mounted on aluminum pins and frozen in liquid nitrogen. Ultrathin cryosections were picked up in a mixture of sucrose and methyl cellulose. Rabbit polyclonal antibody against syntaxin 7 was visualized by binding to protein A-gold. To increase the immunostaining for syntaxin 8, an incubation step with swine anti-rabbit-IgG (Nordic Immnological Laboratories, Tilburg, The Netherlands) was performed after labeling with the primary rabbit polyclonal antibody. Mouse derived anti-TfR and

clathrin antibodies were visualized in a two-step procedure using rabbit anti-mouse IgG antibody (Dako, Glostrup, Denmark) to provide binding sites for protein A-gold.

To establish the distribution pattern of syntaxin 7 and syntaxin 8, areas of the grids were selected that contained cells exhibiting a good ultrastructure. At a magnification of 25,000× these areas were scanned along a fixed track, and all gold particles within a distance of 30 nm from a membrane were counted as positive and assigned to the compartment over which they were located. For syntaxin 7 this procedure was performed in sections double immunolabeled for clathrin, and syntaxin 7-positive membranes were also scored for the presence of clathrin label. Syntaxin 8 labeled only weakly in double-labeled sections, and quantitations for this SNARE were therefore performed in single-labeled grids.

Quantitations were done in CHO (syntaxin 7) and PC12 (syntaxin 8) cells. The various compartments were defined by strict morphological criteria. Tubulovesicular membranes at the *trans* side of the Golgi or near endosomes were considered as *trans*-Golgi network (TGN) and endosome-associated tubulovesicles, respectively. Tubulovesicular membranes that were not associated with Golgi or endosomes were designated as tubulovesicles per se. A measure of the maturation stage of an endosomal vacuole is the number of vesicles enclosed (Geuze, 1998). Thus, EEs, LEs, and lysosomes could therefore be defined by shape and content. EEs were elongated vacuoles positive for TfR with few internal vesicles. LEs were more globularly shaped and contained numerous internal vesicles. Lysosomes had an electron-dense content with occasional membrane remnants.

In CHO cells, a considerable percentage of syntaxin 7 label was found on PM-associated vesicles but not internal vesicles or tubular extensions. When the cells were incubated for 60 min at 37°C with BSA-gold conjugated to 5-nm colloidal gold (Slot *et al.*, 1988), these vesicles contained the tracer, which defined them as primary endocytic vesicles.

RESULTS

Syntaxin 7 and Syntaxin 8 Are Ubiquitously Expressed

Defining the expression patterns and localization of the various members of the syntaxin family is an important step in understanding the specific functions of these proteins. Since its initial characterization, syntaxin 7 has been suggested to reside in lysosomes and LEs (Wang *et al.*, 1997) as well as EEs (Wong *et al.*, 1998a); thus its localization remains controversial. To more fully analyze syntaxin 7 localization and function, we raised a polyclonal antibody against its cytosolic domain. After affinity purification, in Western blots the antibody recognized a major single band of ~39 kDa in HeLa cell PNS (Figure 1A, first lane). The same size band was also detected in PNS of several cell lines tested (Figure 1B), in agreement with the earlier observation that syntaxin 7 is ubiquitously expressed (Wong *et al.*, 1998a). Despite the predicted mass of ~30 kDa, on SDS-PAGE syntaxin 7 runs as an apparent 39-kDa protein. Because syntaxin 7 is 53% identical to syntaxin 13, we tested our affinity-purified antibody for cross-reactivity between these proteins. This 39-kDa band was blocked by preincubating the antibody with 1 μg/ml recombinant syntaxin 7 (Figure 1A, second lane) but not by preincubating with 1 μg/ml recombinant syntaxin 13 (Figure 1A, third lane). Similarly, a syntaxin 13-specific band could be blocked with recombinant syntaxin 13 but not syntaxin 7. From these results we conclude that anti-syntaxin 7 and anti-syntaxin 13 antibodies are specific for their corresponding antigens.

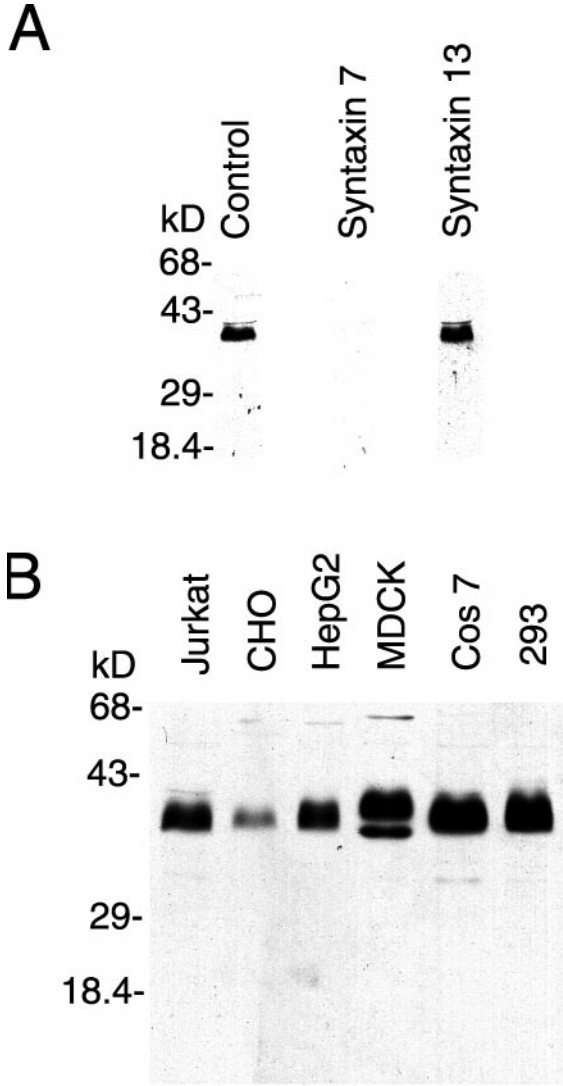

Figure 1. Syntaxin 7 is a broadly expressed SNARE. (A) A rabbit polyclonal anti-syntaxin 7 antibody recognizes a major 39-kDa band in HeLa cell PNS (control). This band represents endogenous syntaxin 7, because it can be blocked with 1 μg/ml recombinant syntaxin 7 (syntaxin 7) but not 1 μg/ml recombinant syntaxin 13 (syntaxin 13). (B) PNSs from Jurkat, CHO, HepG2, Madin–Darby canine kidney, Cos7, and 293 cell lines were analyzed using the anti-syntaxin 7 antibody. A single major 39-kDa band is detected in every cell line investigated.

We previously determined the localization of myc-tagged syntaxin 8 transiently expressed in NRK cells (Steegmaier *et al.*, 1998). To determine the localization of endogenous syntaxin 8, we generated rabbit polyclonal antibodies against the syntaxin 8 H3 domain (aa 141–216). As predicted from the syntaxin 8 sequence, the anti-syntaxin 8 antibody recognized a major single band of 28 kDa on Western blots (Figure 2). To analyze the tissue distribution pattern of syntaxin 8, affinity-purified antibodies were used on Western blots of a variety of rat tissues, including brain, heart, kidney, liver, lymphnode, skeletal muscle, spleen, and thymus.

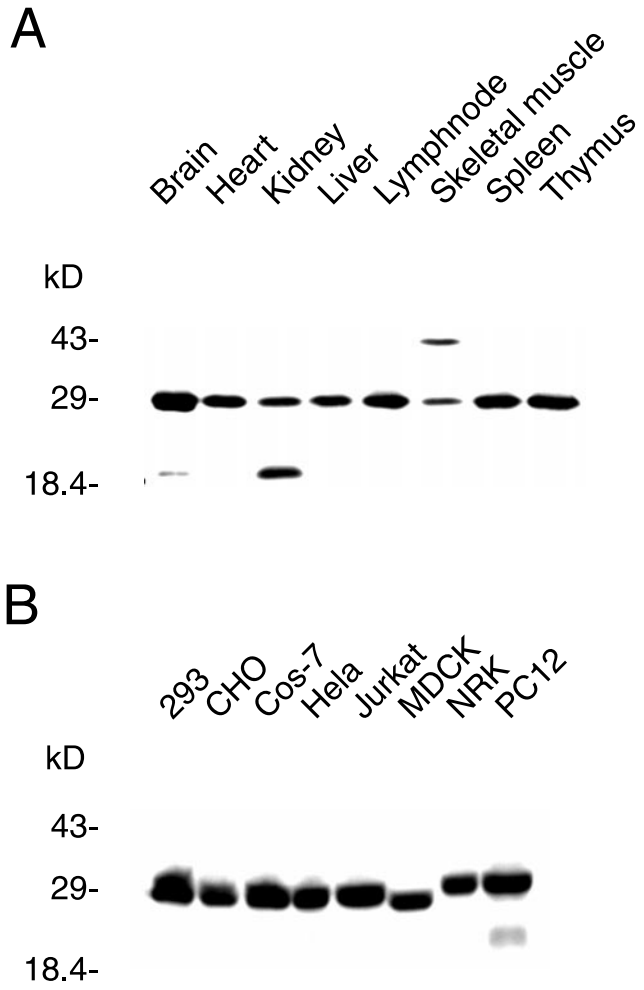

Figure 2. Syntaxin 8 is a broadly expressed SNARE. (A) Multiple-tissue Western blot using the polyclonal anti-syntaxin 8 antibody as described in MATERIALS AND METHODS. (B) Eight cell line extracts were probed with the polyclonal anti-syntaxin 8 antibody. A 28-kDa band is recognized in all cell lines and tissues.

In agreement with the Northern blot results (Steegmaier *et al.*, 1998), syntaxin 8 protein is expressed in all the tissues tested as a major single band (Figure 2A). An additional band of 19 kDa was also detected in both brain and kidney, probably representing syntaxin 8 degradation product. However, we cannot discount the possibility that this band represents a cross-reacting protein species. In skeletal muscle another immunoreactive species of ~43 kDa was detected. This band could represent an alternatively spliced isoform, a post-translational modification, or a distinct cross-reactive protein species that is present only in skeletal muscle. Consistent with the tissue distribution data, syntaxin 8 was also detected in all the different cell lines tested (Figure 2B), suggesting a ubiquitous membrane trafficking function of syntaxin 8. Interestingly, in NRK and PC12 cell lines syntaxin 8 has a slightly higher apparent molecular mass. This is most likely attributable to species differences, because both of these cell lines are derived from rat tissues.

Syntaxin 7 Subcellular Distribution

To determine whether syntaxin 7 is localized early or late in the endosomal pathway, we compared its immunofluorescence pattern with that of LAMP1, a LE and lysosomal marker, as well as TfR, a marker for EEs and REs. In agreement with a previous report (Wong *et al.*, 1998a), syntaxin 7 showed little colocalization with LE and lysosomal markers and a substantial, but not complete, overlap with TfR (Figure 3, A–F). Interestingly, syntaxin 13, a SNARE involved in trafficking via REs, also exhibits a very similar subcellular distribution (Prekeris *et al.*, 1998). Because of the amino acid similarity of syntaxin 7 and 13, both these proteins might be expected to function in a similar pathway. Syntaxin 13 resides mostly in tubulovesicular REs and tubular extensions of EEs where it colocalizes with TfR (Prekeris *et al.*, 1998). To more fully understand the localization of syntaxin 7 we stained NRK and Cos7 cells with anti-syntaxin 7 antibodies and compared its localization with that of syntaxin 13. Because the antibodies against syntaxin 7 and syntaxin 13 were both raised in rabbit, we could not use them for costaining in the same cell. Instead we used Cos7 cells transiently transfected with a GFP-tagged version of syntaxin 13 (Figure 4B). Syntaxin 13-GFP has previously been reported to localize and behave as endogenous syntaxin 13 (Chao *et al.*, 1999; Prekeris, Foletti, and Scheller, unpublished data); thus it could be used to determine its colocalization with syntaxin 7. Also, although syntaxin 7 to a large extent colocalized with syntaxin 13, there were some apparent differences in the cell periphery (Figure 4, A–C). Although syntaxin 13 exhibited a predominantly perinuclear staining, characteristic of REs (Figure 4B), syntaxin 7 was much more widely scattered throughout the cell, with the organelles in the periphery largely lacking syntaxin 13 (Figure 4, A–C). To confirm that these differences in localization of syntaxin 7 and syntaxin 13 were not due to the overexpression of syntaxin 13-GFP, we used anti-syntaxin 13 antibodies to stain NRK cells transiently transfected with syntaxin 7-GFP fusion protein. As in the case of syntaxin 13-GFP fusion protein (Chao *et al.*, 1999), a GFP tag was attached to the C terminus of syntaxin 7. Unpublished data from our laboratory show that syntaxin 7-GFP fusion protein was efficiently inserted into the membranes and exhibited subcellular localization indistinguishable from the endogenous syntaxin 7. Moreover, syntaxin 7-GFP fusion protein also responded to brefeldin A (BFA) and nocodazole treatment in the manner similar to the endogenous syntaxin 7, suggesting that syntaxin 7 fusion protein correctly localizes in NRK and Cos7 cells. Once again, endogenous syntaxin 13 and syntaxin 7-GFP showed only a partial overlap (Figure 4, D–F). These data suggest that syntaxin 7 and 13 are involved in a different trafficking step through the same or closely related organelles.

The dynamics of membrane proteins in the presence of BFA and nocodazole can reveal features of their native localization and trafficking patterns. BFA causes a block in endoplasmic reticulum (ER) to Golgi trafficking as well as tubulation of TGN and endosomal membranes (Robinson and Kreis, 1992). Eventually, the TGN and endosomes collapse into a continuous network, which accumulates around the microtubule-organizing center (Lippincott-Schwartz *et al.*, 1991). The microtubule-depolymerizing agent nocodazole, on the other hand, blocks the protein exit from EEs as

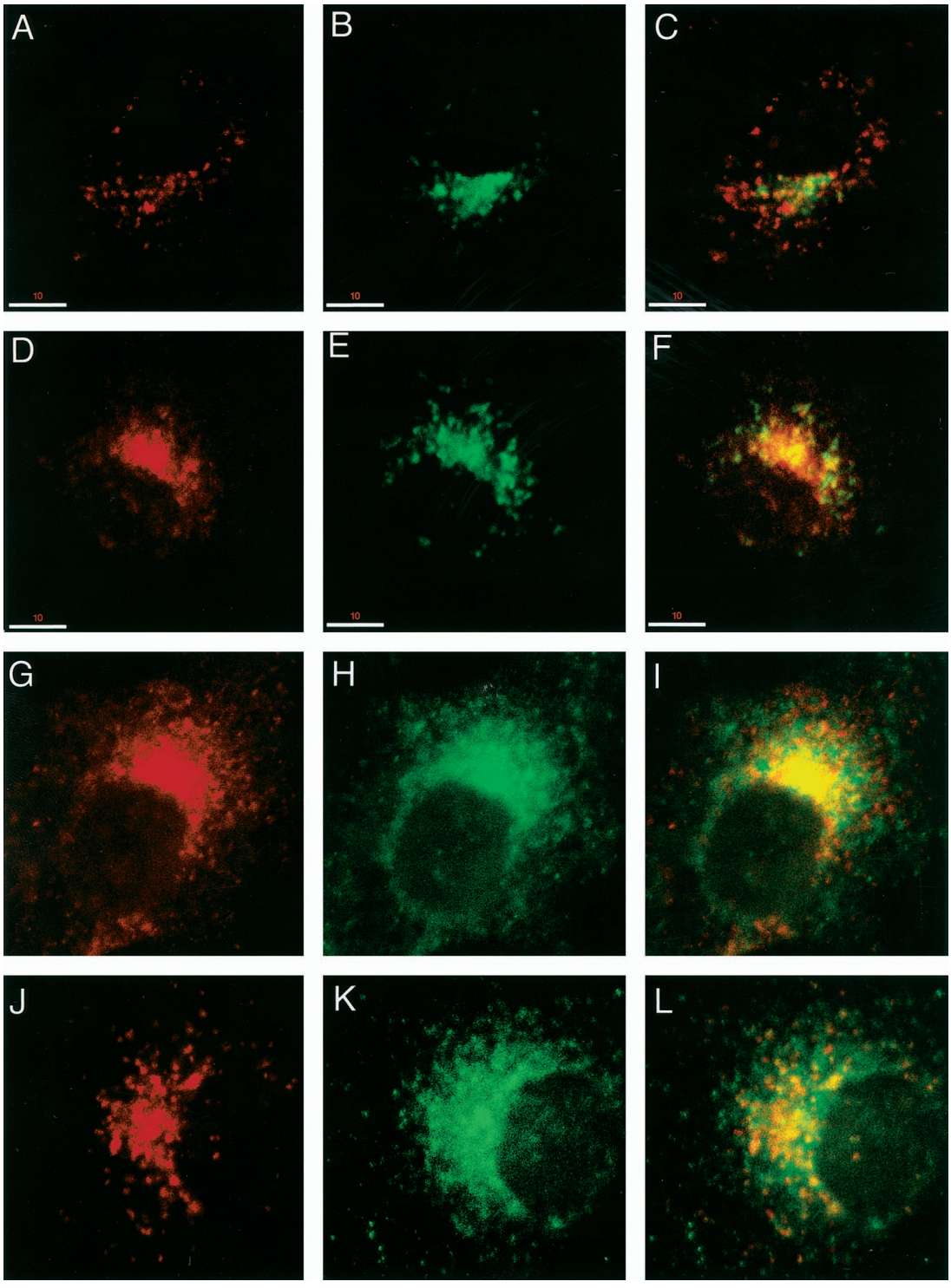

Figure 3. Syntaxin 7 and 8 partially colocalize with the endosomal markers in Cos-7 cells. Cos-7 cells were fixed, permeabilized, and stained with the following antibodies: anti-syntaxin 7 (B and E), anti-syntaxin 8 (H and K), anti-TfR (D and G), anti-LAMP 1 (A and J). (C, F, I, and L) Merged images. Yellow represents areas of overlap. Bar, 10 μm.

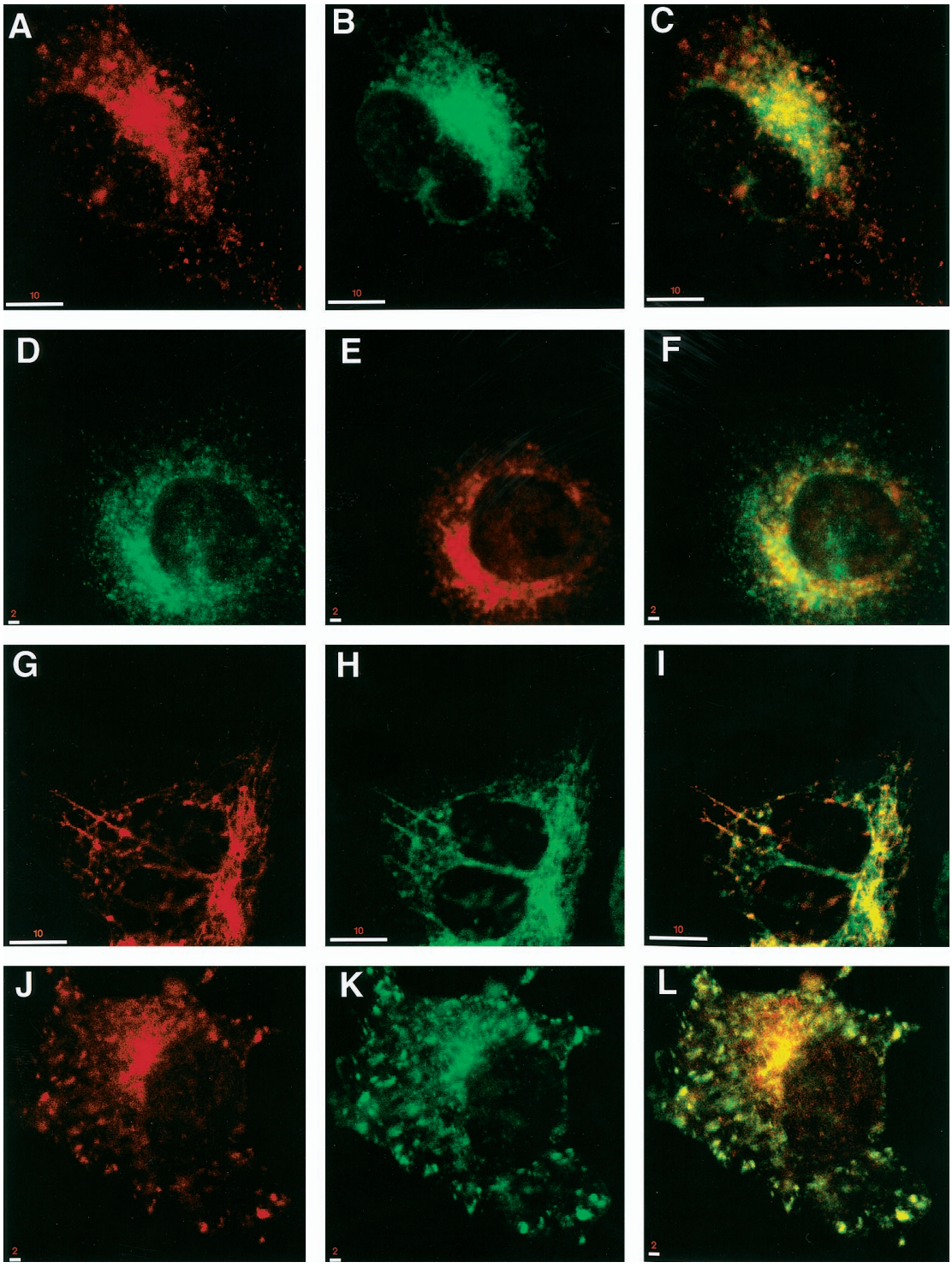

Figure 4. Syntaxin 7 and 13 are localized in overlapping endosomal compartments. Cos7 cells expressing syntaxin 13-GFP (B, H, and K) and NRK cells expressing syntaxin 7-GFP (D) were immunostained for syntaxin 7 (A, G, and J) or syntaxin 13 (E). GFP was visualized using filters for FITC (B, D, H, and K). Before fixing some cells were treated with 5 μg/ml BFA for 15 min (G–I) or with 5 μg/ml nacodazole for 30 min (J–L). Yellow represents areas of overlap in merged images (C, F, I, and L). Bars: A–C and G–I, 10 μm; D–F and J–L, 2 μm.

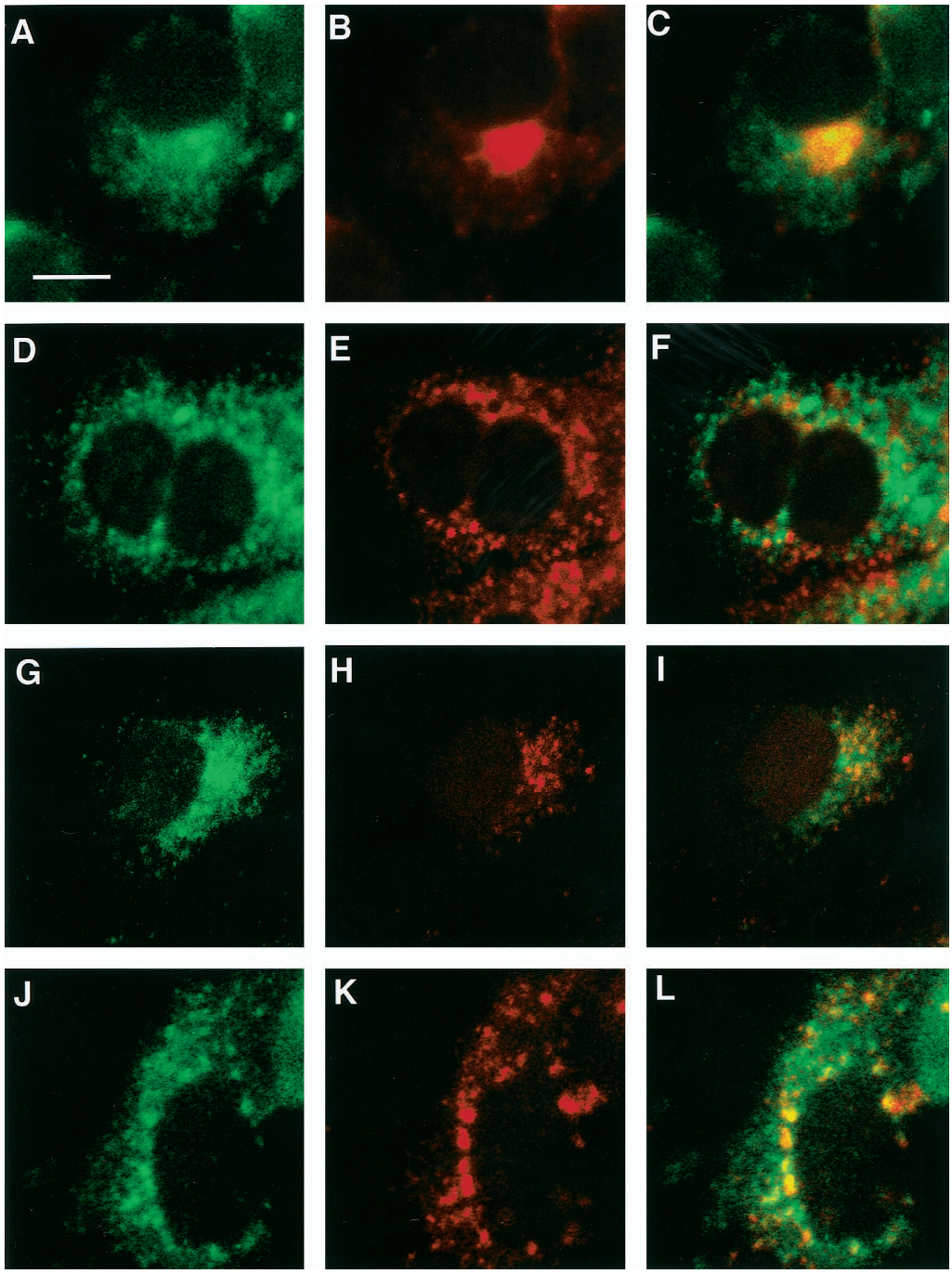

Figure 5. Localization of syntaxin 8 in BFA- and nocodazole-treated Cos 7 cells. Cos 7 cells were treated with 5 μg/ml BFA for 15 min (A–C and G–I) or with 5 μg/ml nocodazole for 30 min (D–F and J–L), followed by staining for syntaxin 8 (A, D, G, and J), TfR (B and E), and LAMP 1 (H and K). (C, F, I, and L) Merged images. Yellow represents areas of overlap in merged images. Bar, 10 μm.

well as inhibiting protein trafficking to lysosomes (Yamashiro *et al.*, 1984). Thus, we used BFA and nocodazole to further understand the extent of syntaxin 7 and 13 overlap. As previously reported (Prekeris *et al.*, 1998; Wong *et al.*, 1998a), treatment of the NRK cells with BFA or nocodazole resulted in tubulation and accumulation of syntaxin 7- and 13-labeled membranes in large vesicular structures, respectively (Figure 4, G–L). Note that after BFA and nocodazole treatment syntaxin 7 still colocalizes with syntaxin 13 to a great extent (Figure 4, G–L). Thus, although the function of syntaxin 7 still remains to be determined, its subcellular localization suggests that both syntaxin 7 and 13 might

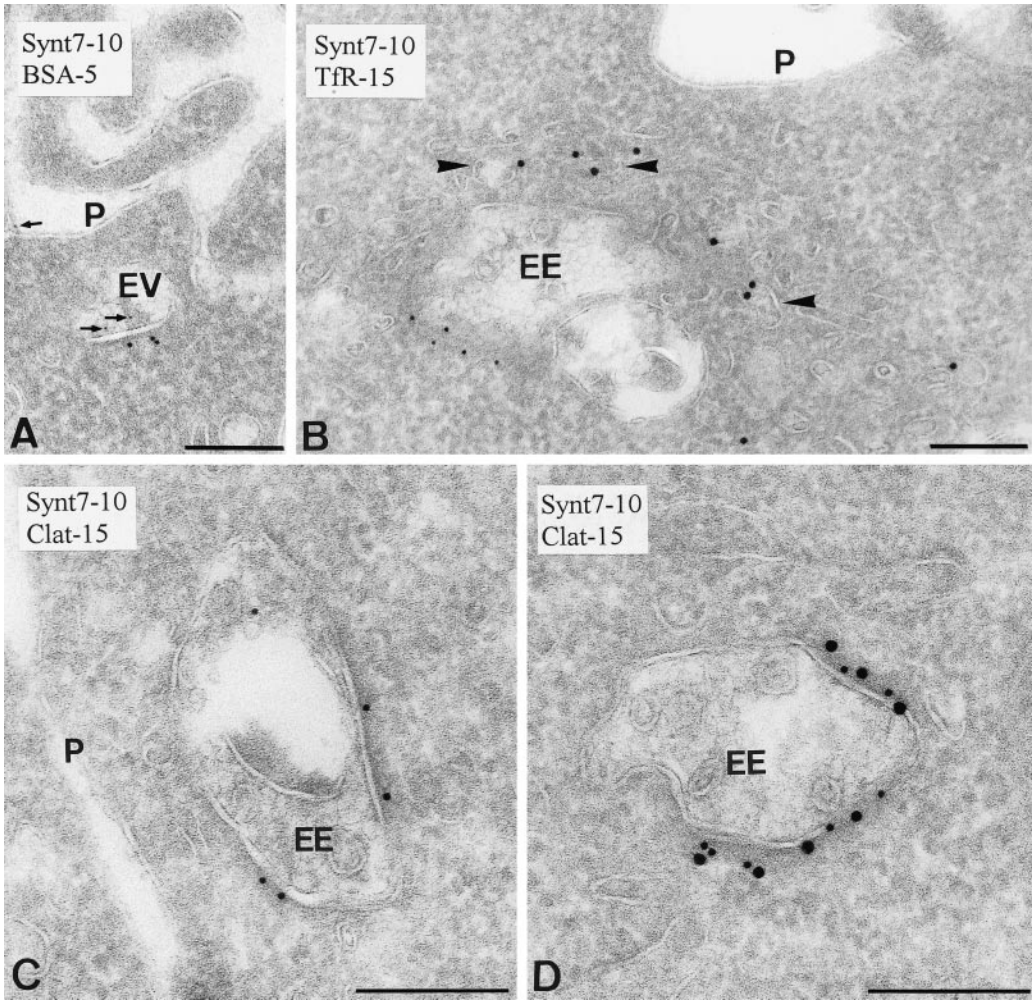

Figure 6. Immunogold labeling of syntaxin 7 on ultrathin cryosections of CHO cells. (A) CHO cells were incubated for 60 min at 37°C with BSA–5-nm gold (arrows). Syntaxin 7 is found on a part of an endocytic vesicle (EV) with a dense cytosolic coat. (B) Syntaxin 7 is present on an EE vacuole, with TfR (15 nm gold) in the EE-associated tubulovesicles. (C and D) EEs of CHO cells double immunogold labeled for syntaxin 7 and clathrin (15-nm gold). C and D show two examples from the same grid. Dense cytosolic areas of EE vacuoles stain positive for syntaxin 7. In approximately two-thirds of the EEs (see Table 1) this coat also stains for clathrin. P, PM. Bars, 200 nm.

function in the same pathway, perhaps in a sequential manner.

Subcellular Distribution of Syntaxin 8

To ascertain the localization of endogenous syntaxin 8 protein, we performed immunofluorescence studies on various cell lines with the antibody characterized in Figure 2. It has been previously reported that epitope-tagged transiently transfected syntaxin 8 is localized in the ER of NRK cells (Steegmaier *et al.*, 1998). Unexpectedly, in Cos7 cells endogenous syntaxin 8 seemed to be distributed in a punctate pattern (Figure 3, H and K) more similar to post-Golgi staining rather then ER staining. A similar staining pattern was also observed in NIH3T3 and HeLa cells. To gain further insight into the intracellular localization of endogenous syntaxin 8, we compared its immunostaining pattern with those of well-characterized markers of the endosomal, and lysosomal compartments. Syntaxin 8 showed a partial colocalization with TfR (Figure 3, G–I) and LAMP 1 (Figure 3, J–L), EE/RE and LE/lysosomal markers. In addition, unpublished data from our laboratory show that syntaxin 8 also partially overlaps with syntaxin 6, a known TGN protein. These data suggest that syntaxin 8 resides in TGN, EE, and LE compartments. It is unclear why epitope-tagged transfected syntaxin 8 is localized differently from the endogenous protein, particularly because localization of the vast majority of transfected SNARE proteins closely matches the localization of their endogenous counterparts.

In contrast to syntaxin 7, BFA treatment did not affect the distribution of syntaxin 8 (Figure 5, A and G). Although BFA caused the accumulation of TfR around the microtubule-organizing center (Figure 5B), little or no effect was observed on the distribution of organelles containing syntaxin 8 (Fig-

Table 1. Syntaxin 7 is enriched in vacuolar EEs

Compartment	Percentage of total gold	No. of gold particles counted
Golgi complex	3 ± 1.2	13
Plasma membrane	7 ± 2.4	28
Clathrin coated pits at PM	0 ± 0	3
Tubulovesicles		
Clathrin coated	4 ± 1.6	15
Noncoated	11 ± 3.7	42
Vacuolar EEs	50 ± 4.2	191
Clathrin coated	34 ± 3.4	130
Non–clathrin coated	15 ± 2.9	57
Noncoated	1 ± 0.9	4
EE-associated tubules	2 ± 0.5	9
Endocytic vesicles	21 ± 4.5	83
Clathrin coated	10 ± 4.9	40
Non–clathrin coated	11 ± 5	43

Ultrathin cryosections of CHO cells were double immunogold labeled for syntaxin 7 and clathrin. Quantitations were performed in three counting sessions, and for each counting session the percentage of total gold particles found over a specific compartment was calculated. The numbers in the first column represent the means of these three sessions ± SD.

ure 5, A and G) or LAMP 1 (Figure 5H). In contrast to BFA, nocodazole treatment resulted in redistribution of syntaxin 8 to large organelles scattered throughout the cytoplasm (Figure 5, D and J). Although many of these organelles probably represent enlarged EEs, at least some of them are likely to be LEs, because they contain LAMP1 (Figure 5K) but are devoid of TfR (Figure 5E). Thus, the immunolocalization data suggest a possible involvement of syntaxin 8 in the LE–lysosomal pathway.

Syntaxin 7 Is Localized to Endocytic Vesicles and the Vacuolar EE

The subcellular distribution of syntaxin 7 was analyzed in more detail by immunogold labeling of ultrathin cryosections and electron microscopy. The highest labeling density was obtained in CHO cells (Figure 6, A–D), which were therefore chosen for quantitative analysis (Table 1), but essentially similar labeling patterns were observed in PC12, Madin–Darby canine kidney, and HepG2 cells. The majority of syntaxin 7 labeling was found in endocytic vesicles and EEs (Figure 6 and Table 1). In EEs, syntaxin 7 was mostly restricted to the EE vacuole, in contrast to TfR, which prevailed in EE-associated tubulovesicles (Figure 6B). Remarkably, syntaxin 7 label in endocytic vesicles and EEs often occurred on those parts of a membrane that showed an electron-dense coat at the cytoplasmic side (Figure 6, C and D). This accumulation of syntaxin 7 in coated membranes was specific for endocytic vesicles and EEs and not observed at the PM. To investigate the nature of this coat, cells were double labeled for syntaxin 7 and clathrin. As shown in Figure 6D, syntaxin 7 colocalized with clathrin in coated areas of EE membranes. However, clathrin was not always detected in these coats (Figure 6C). Quantitative analysis showed that practically all EE- and endocytic vesicle-associated syntaxin 7 was found in coated membranes, 50–75% of which were also labeled for clathrin (Table 1).

Additional low, but significant, labeling was also found on the PM and in clathrin-coated and noncoated tubulovesicles (Table 1). The latter two types of vesicles are most likely transport intermediates involved in shuttling syntaxin 7 between EEs and the PM.

Syntaxin 8 Is Localized to Noncoated Golgi- and Endosome-associated Vesicles and Endosomes

The subcellular localization of syntaxin 8 was studied in PC12 and Cos7 cells. Both cells exhibited a low but essentially similar labeling (Figure 7). Unlike syntaxin 7, syntaxin 8 was not confined to a specific compartment. Labeling was found on TGN membranes, endosomes, and numerous tubulovesicles dispersed throughout the cytoplasm or in close vicinity to endosomes. Notably, most syntaxin 8-positive membranes lacked a clathrin coat (Figure 7 and Table 2), indicating that syntaxin 8 travels to endosomes via a non–clathrin-mediated pathway. This notion was reinforced by the absence of syntaxin 8 from secretory granules of PC12 cells (Table 2) and consistent with the apparent lack of BFA effect on syntaxin 8 distribution (Figure 5).

Syntaxin 8 was found in both early and late endocytic compartments (Figure 7). Quantitation of this distribution in PC12 cells revealed approximately similar percentages of syntaxin 8 in EEs, LEs, and lysosomes (Table 2). In EEs and LEs, syntaxin 8 distributed approximately equally over vacuole and associated tubulovesicles. Approximately 20% of the labeling in PC12 cells was found on noncoated tubulovesicles with an appearance similar to those found in TGN and near endosomes. Possibly, these vesicles are involved in TGN–endosome or intraendosome trafficking.

Syntaxin 7 Actively Cycles through the PM

Immunolocalization data suggest that syntaxin 7 is a SNARE involved in protein trafficking through the vacuolar EEs. One of the possible syntaxin 7 functions is mediating endocytic vesicle fusion with EEs. Alternatively, syntaxin 7 might be involved in transporting membrane proteins back to the PM from EE vacuoles. The "fast" protein recycling from EEs, bypassing the REs, has been recently reported and seems to involve a separate trafficking pathway, because it has different kinetic properties compared with "slow" protein recycling (Schmid, 1988; Sheff *et al.*, 1999). To test these possibilities we used an antibody uptake assay to determine whether syntaxin 7 is actively cycling to the PM. Because most syntaxins do not contain a large enough luminal domain for antibody uptake assays, we used cells transiently transfected with syntaxin 7-GFP, rbet1-GFP, or syntaxin 13-GFP fusion proteins. Upon insertion of syntaxin-GFP constructs into the membrane, GFP is situated within the lumen of the appropriate organelle (Chao *et al.*, 1999). Thus, after exocytosis the GFP would be exposed on the surface for the interactions with anti-GFP antibody in the media. Incubation of syntaxin 7-GFP–expressing NRK cells with anti-GFP antibody resulted in efficient labeling of cells, indicating that syntaxin 7 does cycle through the cell surface (Figure 8, J, L, and M). The antibody uptake was dependent on protein cycling through the PM, because cells expressing rbet1-GFP, a known ER-to-Golgi SNARE, did not uptake the anti-GFP

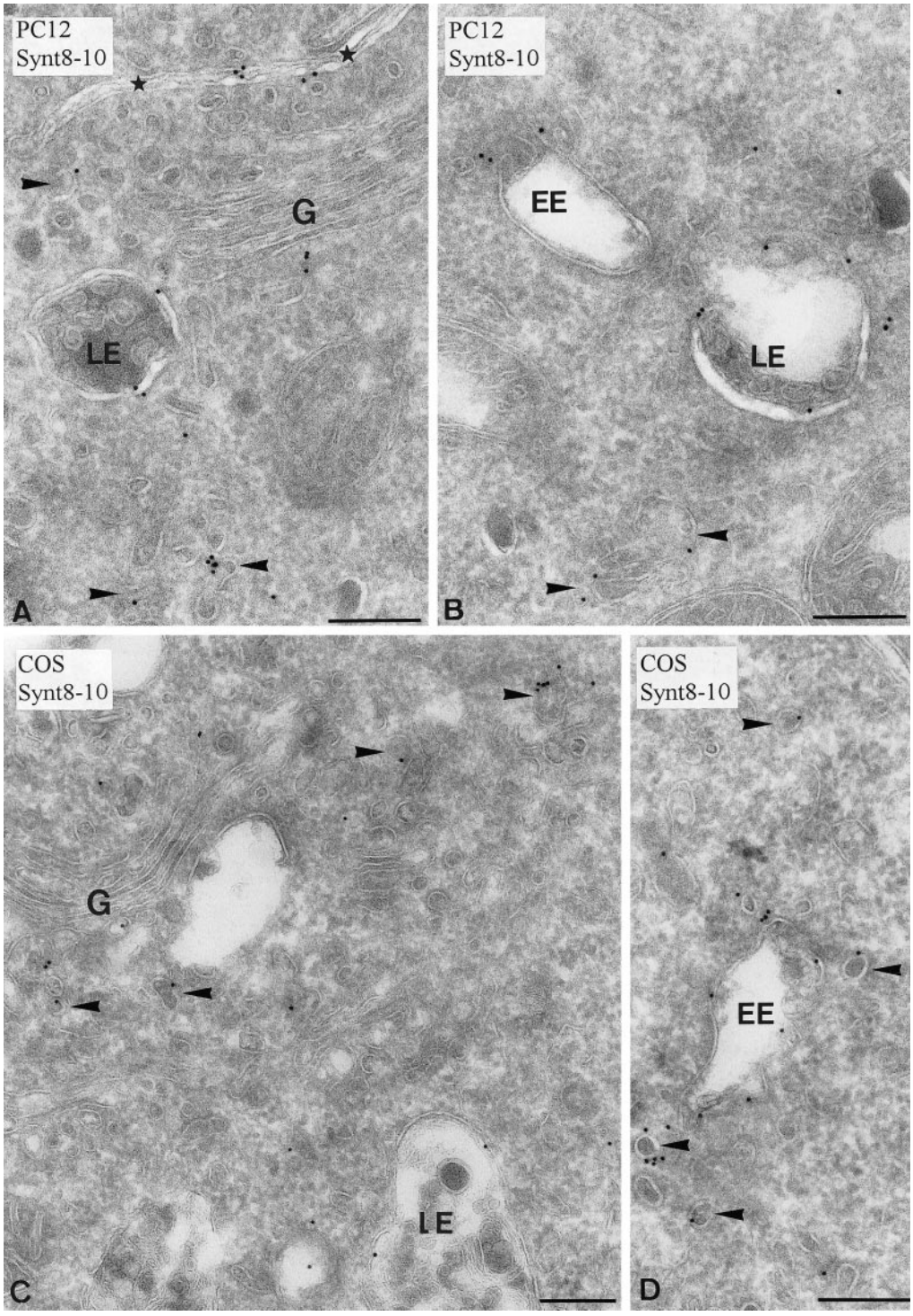

Figure 7. Immunogold labeling of syntaxin 8. Ultrathin cryosections of PC12 (A and B) and Cos7 (C and D) cells were immunolabeled with anti-syntaxin 8 (10-nm gold). Syntaxin 8 is found in TGN membranes (A, asterisk), the vacuolar membrane of EEs and LEs, and numerous noncoated tubulovesicles (arrowheads) near the Golgi and endosomes but also dispersed in the cytoplasm. G, golgi. Bars, 200 nm.

Table 2. Syntaxin 8 is localized to noncoated TGN membranes and tubulovesicles

Compartment	Percentage of total gold	No. of gold particles counted
ER	8 ± 2.5	46
Golgi complex	4 ± 0.8	21
TGN	31	180
Clathrin coated	1 ± 1.2	7
Noncoated	30 ± 5.1	173
Tubulovesicules		
Clathrin coated	2 ± 1.9	11
Noncoated	19 ± 4.6	110
EEs	8 ± 2.5	47
LEs	10 ± 4.8	57
Lysosomes	15 ± 1.5	86
PM	1 ± 0.4	9
Clathrin-coated pits	2 ± 1.1	10
Secretory granules	0	5

Ultrathin cryosections of PC12 cells were immunogold labeled for syntaxin 8, swine anti-rabbit, and protein A-gold. Quantitations were performed in four counting sessions, and of each counting session the percentage of total gold particles found over specific compartment was calculated. The numbers in the first column represent the means of these four sessions ± SD. TGN was defined as tubulovesicular membranes at the *trans* side of the Golgi stack.

antibody (Figure 8, B and D). Because the uptake assay was done in the presence of protein synthesis inhibitor cycloheximide, we could exclude the possibility of the antibody uptake during the delivery of newly synthesized syntaxin 7 to the PM for the further sorting. To determine the rates of syntaxin 7 cycling we incubated cells transfected with syntaxin 7-GFP for varying periods with anti-GFP antibody (Figure 8M). The antibody uptake assay confirms that syntaxin 7 cycles through the PM with the $t_{1/2}$ of ~140 min (Figure 8M). Note, however, that the rate of syntaxin 7 cycling measured in this assay is probably somewhat underestimated, because the overall antibody uptake is a combination of the rates of syntaxin 7 recycling and antibody binding. Indeed, the anti-GFP antibody binding $t_{1/2}$ was equal to ~20 min at 37°C (see MATERIALS AND METHODS). Nevertheless, even taking antibody binding rates into account, syntaxin 7 cycling through the PM is much slower than would be expected for a protein involved in fast recycling from the EE, because these half-lives are estimated to be only 5 min. We suggest that syntaxin 7 most likely cycles through the PM via REs rather than the fast recycling pathway. Indeed, although syntaxin 7 is enriched in vacuolar EEs and endocytic organelles, ~11% is present in tubulovesicular REs. Thus, it is tempting to speculate that upon maturation of EEs to LEs, syntaxin 7 is removed from endosomal membranes and recycled back to EEs via PM.

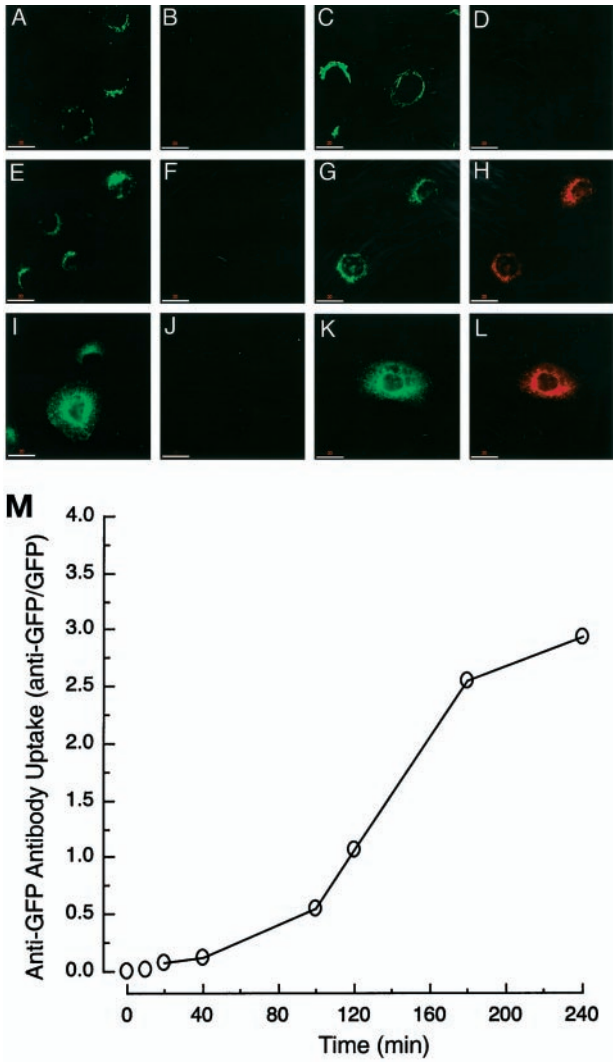

Figure 8. Syntaxin 7 actively cycles through the PM. (A–L) NRK cells were transiently transfected with rbet1-GFP (A–D), syntaxin 13-GFP (E–H), or syntaxin 7-GFP (I–L). Twenty-four hours after transfection cells were incubated for 0 min (A, B, E, F, I, and J) or 100 min (C, D, G, H, K, and L) with 5 μg/ml anti-GFP rabbit polyclonal antibody, followed by fixing and staining them with anti-rabbit IgG conjugated with TxR. TxR (B, F, J, D, H, and L) or GFP (A, C, E, G, I, and K) fluorescence was then visualized using confocal microscopy. (M) To obtain the rates of recycling, the NRK cells expressing syntaxin 7-GFP were incubated with anti-GFP antibodies for varying periods. To normalize for the differences in recombinant protein expression, TxR fluorescence was divided by GFP fluorescence values for every individual cell. Each time point represents the mean of at least eight randomly chosen cells.

Syntaxins 7 and 8 Form Stable and NSF/α-SNAP-sensitive Protein Complexes

The association of syntaxin and VAMP is believed to be the vital step in mediating membrane fusion. Indeed, most syntaxin–VAMP complexes display very high stability, a property that presumably reflects the ability of complex formation to overcome the membrane–membrane repulsion during fusion (Fasshauer *et al*., 1999; Yang *et al*., 1999). To determine whether syntaxin 7 and syntaxin 8 are also part of membrane fusion complexes, we examined the distribution of both proteins using sedimentation velocity gradients. As shown in Figure 9A, after fractionation of HeLa or CHO cell Triton X-100 extracts on 11–34% glycerol gradients, both

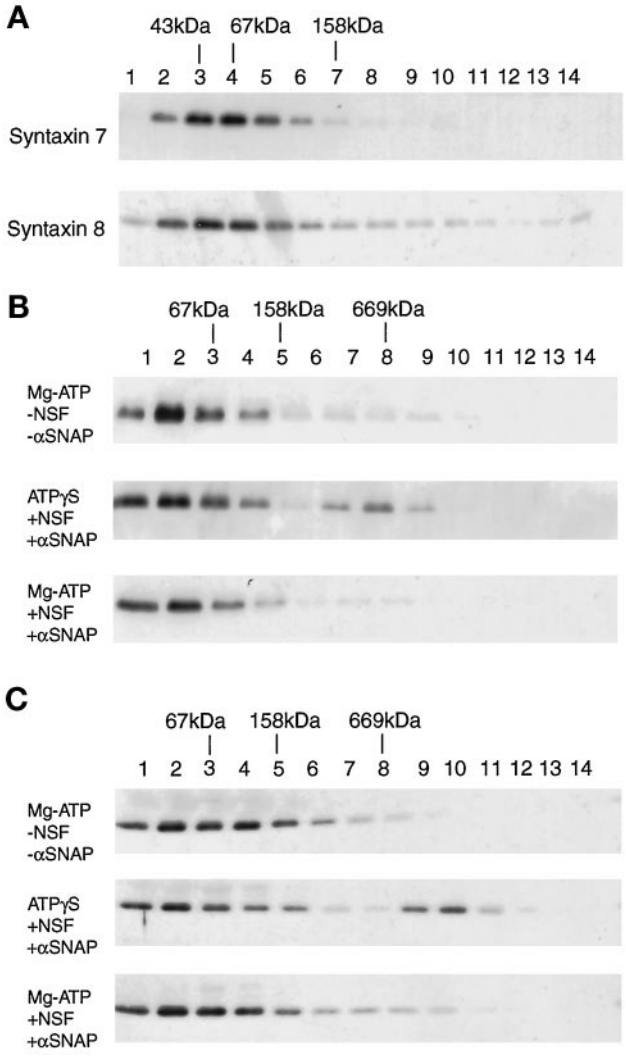

Figure 9. Syntaxin 7 and syntaxin 8 form a complex that is regulated by NSF/α-SNAP. (A) HL-60 cell Triton X-100 extract was fractionated by velocity centrifugation through a 11–34% glycerol gradient. Fractions were separated by SDS-PAGE and analyzed by immunoblotting for the presence of syntaxin 7 (top panel) and syntaxin 8 (bottom panel). (B and C) HL-60 cell Triton X-100 extracts were incubated with (middle and bottom panels) or without (top panel) recombinant NSF and α-SNAP under conditions blocking (middle panel) or allowing (bottom panel) NSF ATPase activity. Extracts were then separated on 23–49% glycerol velocity gradients and blotted for syntaxin 7 (B) and syntaxin 8 (C).

syntaxin 7 and 8 peak at fraction 4, corresponding to an ~67-kDa complex. Part of syntaxin 7 and syntaxin 8 also appears to be in lower-molecular-mass fractions, perhaps corresponding to the monomeric species. Similar results were obtained by separating Triton X-100 extracts on 23–49% glycerol gradients (Figure 9, B and C, top panels).

The fusion core complex consisting of syntaxin, VAMP, and SNAP-25 interacts with NSF and α-SNAP proteins to form a larger complex, which is dissociated by the NSF ATPase upon ATP hydrolysis (Sollner *et al.*, 1993a). To test whether syntaxin 7 and syntaxin 8 protein complexes are also regulated by NSF, we preincubated Triton X-100 extracts with NSF and α-SNAP in the presence of Mg-ATP or ATPγS before separating them on 23–49% glycerol gradients. In the presence of ATPγS a portion of syntaxin 7 and 8 was shifted to fractions 6–8 and 9–11, respectively (Figure 9, B and C, middle panels), consistent with the formation of new complex, which now includes NSF and α-SNAP. As expected, a corresponding reduction in the level of syntaxin 7 and 8 in the region of the 67-kDa complex is noted. Moreover, incubation of Triton X-100 extracts with NSF and α-SNAP under conditions favoring ATP hydrolysis resulted in the accumulation of syntaxin 7 and syntaxin 8 in the slowly sedimenting fractions (Figure 9, B and C, bottom panels).

Syntaxin 8 Functions Early in Protein Trafficking from EEs to LEs

To investigate the role of syntaxin 7 and syntaxin 8 in endosomal recycling and lysosomal degradation, we reconstituted these processes in SLO-permeabilized HeLa cells (Prekeris *et al.*, 1998). The cellular processes required for Tf and EGF trafficking are retained even after cells are permeabilized with SLO. The time course and extent of cytosol-dependent Tf recycling and EGF degradation in SLO-permeabilized cells closely resemble those of intact cells (Prekeris *et al.*, 1998; Advani *et al.*, 1999). Moreover, Tf and EGF trafficking in permeabilized cells is *N*-ethylmaleimide sensitive and ATP dependent (Prekeris *et al.*, 1998; Advani *et al.*, 1999) indicating that this experimental system can be used to address the role of different SNAREs in endosomal trafficking.

To accumulate ^{125}I-Tf and ^{125}I-EGF in EEs, we loaded HeLa cells at 18°C for 1 h. Under these loading conditions most extracellular tracers accumulate in vacuolar EEs, because 18°C incubation blocks the exit from EEs (Futter *et al.*, 1996). To initiate ^{125}I-Tf and ^{125}I-EGF exit from EEs, cytosol was added, and SLO-permeabilized cells were incubated at 37°C. We then used anti-syntaxin 7 and anti-syntaxin 8 antibodies to investigate the role of these proteins in endosomal trafficking. Consistent with the putative role of syntaxin 7 in PM-to-EE trafficking, anti-syntaxin 7 antibodies had no effect on either Tf or EGF trafficking (Figure 10, A and B). Indeed, the SLO-permeabilized assay can only measure protein trafficking from EEs, because the uptake of PM-bound tracers is very rapid. Nevertheless, we cannot exclude the possibility that anti-syntaxin 7 antibodies are simply not capable of blocking syntaxin 7 function in this type of assay.

In contrast to syntaxin 7, the anti-syntaxin 8 antibody reduced cytosol-dependent EGF degradation (Figure 10A). Addition of the anti-syntaxin 8 antibody resulted in up to 55% inhibition of EGF degradation at a concentration of 200 μg/ml (Figure 10C). The inhibition at 100 μg/ml antibody concentration was statistically significant ($p = 0.05$), concentration dependent, and not observed with IgG or anti-syntaxin 6 and 7 antibodies (Figure 10, A and C). Furthermore, unpublished data in our laboratory showed that this inhibition could be reversed by preincubating anti-syntaxin 8 antibodies with 150 μg/ml recombinant syntaxin 8 but not GST proteins. In addition, anti-syntaxin 8 antibodies had no effect on Tf recycling, indicating that its effect is specific for

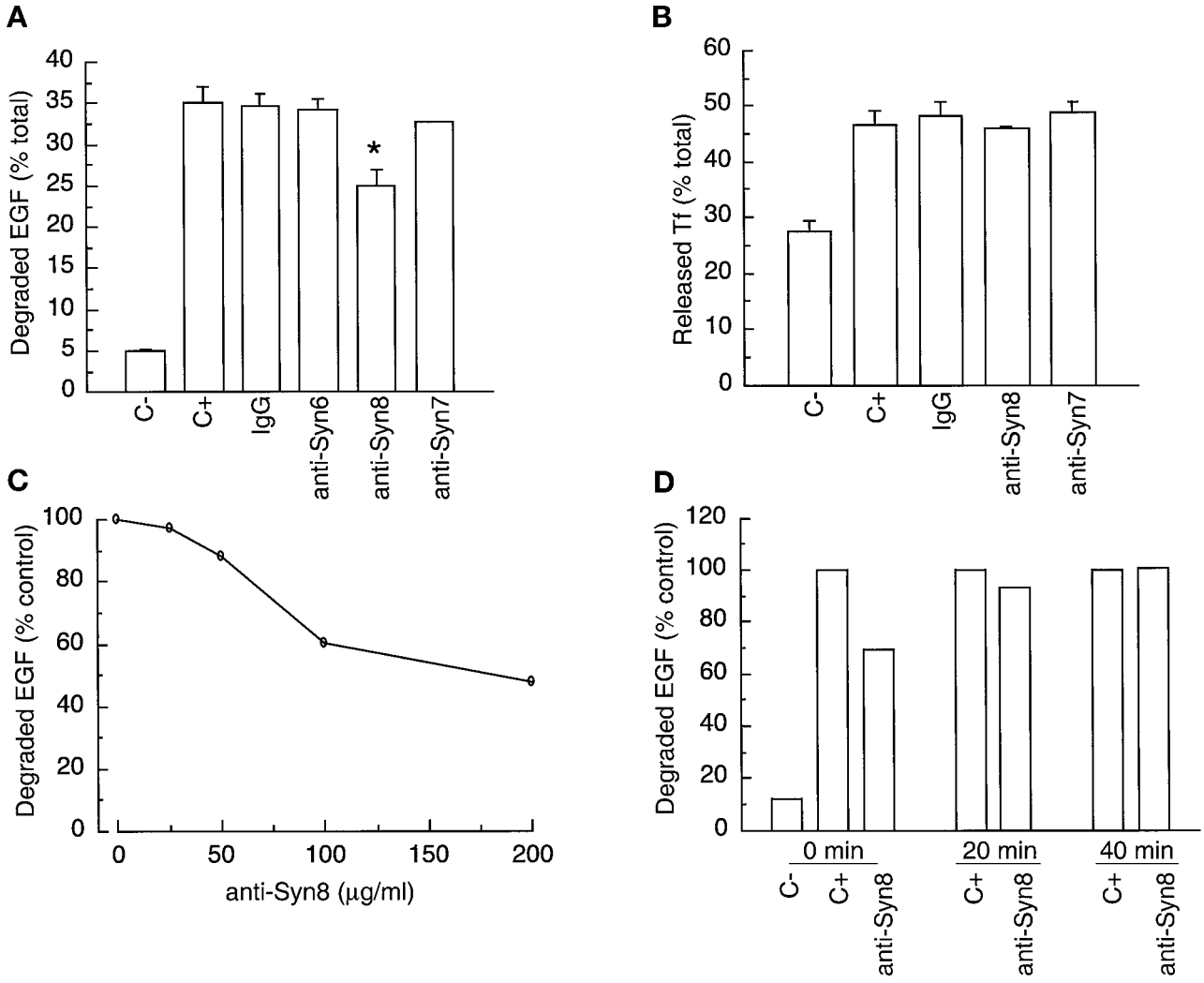

Figure 10. Syntaxin 8 functions in an early step of protein transport from EEs to LEs. Tf and EGF trafficking was measured using an SLO-permeabilized HeLa cell assay as described in MATERIALS AND METHODS. EGF (A) or Tf (B)-loaded and SLO-permeabilized cells were incubated without (C−) or with (remaining samples) cytosol for 2 h at 37°C with 100 μg/ml anti-syntaxin 6 (anti-Syn6), anti-syntaxin 8 (anti-Syn8), anti-syntaxin 7 (anti-Syn7), or rabbit IgG (IgG). The data shown are the means of at least three independent experiments ± SEM An asterisk marks the statistically significant difference at $p < 0.05$. (C) SLO-permeabilized HeLa cells were preincubated with varying concentrations of anti-syntaxin 8 antibody before measuring the EGF degradation. Data are expressed as a percentage of total cytosol-dependent EGF degradation. (D) EGF-loaded HeLa cells were chased for varying amounts of time at 37°C followed by SLO permeabilization. Cells were then preincubated with 100 μg/ml anti-syntaxin 8 antibody and EGF degradation measured as described above. These data are expressed as a percentage of total cytosol-dependent EGF degradation.

the lysosomal pathway (Figure 10B). We interpret these data as demonstrating that syntaxin 8 is involved in a trafficking step needed for EGF transport from EEs to LEs and lysosomes. Because the lysosomal degradation pathway likely involves many different trafficking steps, it remains unclear which precise step is actually mediated by syntaxin 8. In an attempt to address this issue, we chased ^{125}I-EGF-loaded HeLa cells at 37°C for different periods before permeabilizing with SLO and adding anti-syntaxin 8 antibodies. Interestingly, a 40-min chase completely eliminated the effect of anti-syntaxin 8 antibodies on EGF degradation (Figure 10D). Because EGF is almost completely translocated from EEs to LEs within the first 60 min after release from EEs (Futter *et al.*, 1996), our data suggest that syntaxin 8 is probably involved in EGF trafficking from EEs to LEs rather than from LEs to lysosomes.

DISCUSSION

Although the pathways of endosomal recycling and degradation have been extensively characterized, the identity and function of the molecules that mediate this trafficking are only just beginning to be understood. This is partly because

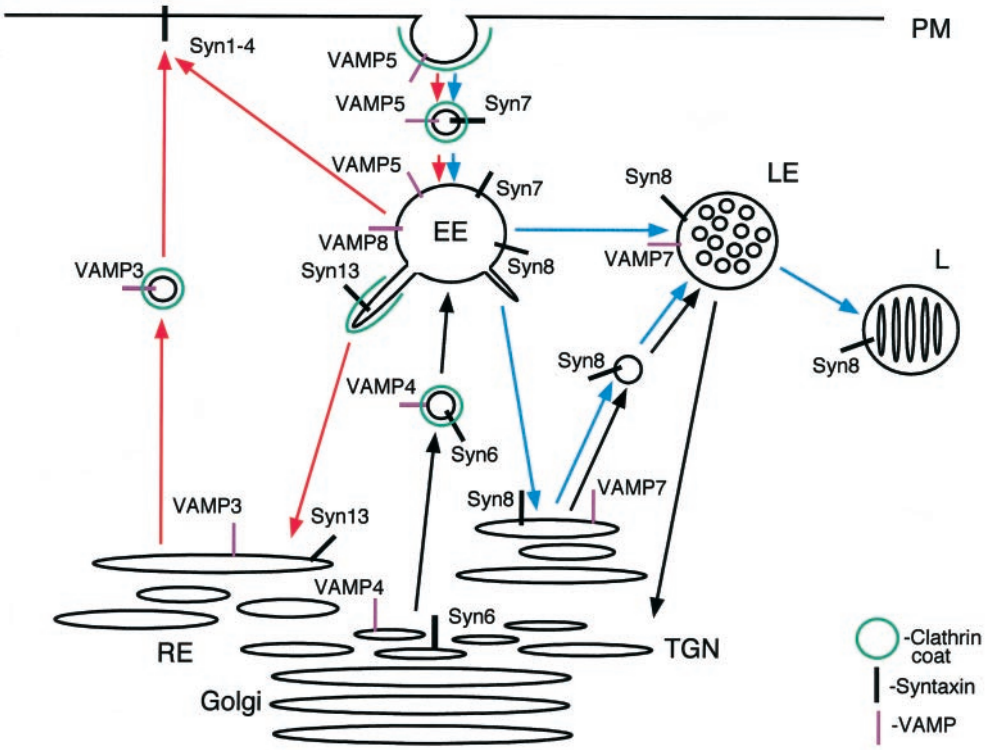

Figure 11. Localization of SNARE proteins within endosomal and lysosomal pathways of the eukaryotic cell. The protein recycling pathway traversed by the TfR is indicated by red arrows. The degradation pathway traversed by the EGFR–EGF complex as it travels to the lysosomes is blue. The protein trafficking from and to the TGN is marked with black arrows. L, lysosomes.

the endocytic organelles are highly dynamic, and their structure is continuously remodeled, making it difficult to appreciate their three-dimensional organization. Furthermore, the dynamic nature of the compartments makes it difficult to define the boundaries between them. The characterization of several endosomal SNAREs (Advani *et al.*, 1998; Steegmaier *et al.*, 1998; Wong *et al.*, 1998a,b; Advani *et al.*, 1999), including syntaxin 7 and syntaxin 8 presented in this work, now allows us to begin to understand the molecular mechanisms involved in the regulation of endocytic trafficking.

Proteins of the VAMP, syntaxin, and SNAP-25 families mediate membrane fusion by pairing across opposite membranes (Hanson *et al.*, 1997; Lin and Scheller, 1997). Many membrane trafficking pathways have been conserved throughout evolution because highly conserved sets of SNAREs are found to localize similarly in the plant and animal kingdoms. Indeed, several mammalian SNAREs, such as syntaxin 5, sec22b, and syntaxin 13, were identified based on their homology to known yeast proteins and appear to mediate similar membrane trafficking steps (Hay *et al.*, 1996; Bock and Scheller, 1997). From this work we propose that, based on sequence similarity, endosomal syntaxins fall into two sets of SNAREs, which are involved in separate pathways of endosomal trafficking.

The first group consists of three mammalian syntaxins: syntaxin 7, syntaxin 13, and syntaxin 16, which form a subfamily based on sequence homology (Steegmaier *et al.*, 1998). All these syntaxins were identified based on their homology to Pep12p, a SNARE that is involved in yeast prevacuolar trafficking (Becherer *et al.*, 1996). Although the function of syntaxin 16 remains to be determined, syntaxin 13 appears to mediate trafficking from EEs to REs (Prekeris *et al.*, 1998). In contrast, syntaxin 7 is proposed to act earlier in endosomal trafficking (Figure 11). Our biochemical and immunolocalization data suggest that cargo retrieved from the PM may require syntaxin 7 for transfer to the vacuolar EE. Although we cannot completely discount the possibility that syntaxin 7 mediates fast trafficking from vacuolar EEs to the PM, our data are less consistent with this hypothesis. The direct transport from vacuolar EEs to the PM is characterized by a fast cycling rate of <15 min (Sheff *et al.*, 1999). Our antibody uptake studies suggest that syntaxin 7 cycles through the PM at a much slower rate, probably because of the recycling of syntaxin 7 molecules through REs. Interestingly, syntaxin 7 is also present in endocytic vesicles. The electron microscopic work presented here defines endocytic vesicles as rounded organelles that can be loaded with BSA-gold and lack emerging tubules or internal vesicles. It is appealing to speculate that syntaxin 7 might also be involved in homotypic endosome–endosome fusion during the formation of EEs.

It remains unclear which VAMP interacts with syntaxin 7 to mediate PM-to-EE transport. The ability of syntaxins to bind multiple VAMPs resulting in complexes with similar stability (Yang *et al.*, 1999) may make it difficult in this case to identify syntaxin binding partners by coprecipitation. Indeed, Western blot analysis of syntaxin 7 immunoprecipitates revealed the presence of several VAMPs, perhaps because of their binding to syntaxin 7 after Triton X-100 extraction. Based on subcellular localization studies, VAMP5 is a candidate for the physiological binding partner for syntaxin 7. VAMP5 is the only endosomal VAMP that is abundant at the PM and also seems to be present in EEs and endocytic vesicles (Zeng *et al.*, 1998).

One of the most fascinating aspects of syntaxin 7 and syntaxin 13 localization is that both proteins are present in the same organelle, yet they are segregated in either vacuolar or tubular parts of EE (Figure 11). Although the mechanisms of syntaxin localization remain to be determined, the segregation of syntaxin 7 and syntaxin 13 at the organelle level almost certainly involves an active sorting event. Perhaps syntaxin 13 is recruited to EE tubules through an interaction with coat proteins. Consistent with this proposal, syntaxin 13 has been shown to be enriched in clathrin-coated membranes (Prekeris *et al.*, 1998). Generation of tubules from EEs seems to involve membrane coats; thus it will be interesting to see whether syntaxin 13 does preferentially interact with some types of coat proteins. An alternative hypothesis is that syntaxin 13 simply follows other membrane proteins into tubular extensions because of the differences in surface-to-volume ratio compared with vacuolar parts of EEs. Thus, to remain in vacuolar EEs, syntaxin 7 would need a retention mechanism that would restrict its movement into EE tubules. Interestingly, the majority of syntaxin 7 is present in stretches of EE vacuole membrane that have a dense cytosolic coating. Although these coated areas always stained positive for syntaxin 7, they showed a more occasional staining for clathrin. The protein composition of this coat remains to be determined. These observations raise the possibility that a non-clathrin coat is involved in retention of membrane proteins in vacuolar endosomes preventing their entry and recycling through REs.

The second group of endosomal syntaxins contains only two known members: syntaxin 6 and syntaxin 8 (Steegmaier *et al.*, 1999). Based on sequence homology and localization, syntaxin 6 may be the homologue of yeast Tlg1p, which mediates transport from the TGN to endosomes (Bock *et al.*, 1997; Holthuis *et al.*, 1998a,b; Klumperman *et al.*, 1998). In this paper we demonstrate that syntaxin 8 may also play a role in membrane trafficking from EEs to LEs. Immunolocalization studies demonstrate that syntaxin 8 is present in EEs, LEs, and tubulovesicles near the Golgi and endosomes and in cytoplasm. These tubulovesicles are distinct from REs, because our immunofluorescence microscopy data show that they do not contain TfR and are not sensitive to BFA treatment. Similar BFA-insensitive compartments have also been reported to contain VAMP7, an endosomal SNARE also involved in EGFR trafficking to lysosomes (Advani *et al.*, 1999). It is tempting to speculate that syntaxin 8/VAMP7-containing non–clathrin-coated tubulovesicles represent a route in parallel to clathrin coat-dependent TGN-to-endosome membrane trafficking (Figure 11). Indeed, the enrichment of syntaxin 6/VAMP4 in clathrin-coated TGN membranes would support the possibility of two independent syntaxin 6/VAMP4- and syntaxin 8/VAMP7-mediated TGN-to-endosome trafficking pathways. Alternatively, syntaxin 8-containing tubulovesicles might be transit organelles used to actively sort and transport membrane proteins, including EGFR, from EEs to LEs. The majority of lysosomal proteins appear to be sorted for lysosomal degradation by removal from the outer membrane of multivesicular bodies to intraluminal vesicles. Nevertheless, some EGF–EGFR complexes do appear to enter tubulovesicular endosomes, from which they can be recycled back to the PM. This possibility is also supported by the dependency of efficient EGF–EGFR recycling on adaptor protein (AP-1, AP-2, and AP-3)–interacting sorting signals, because the deletion of these signals results in increased recycling of EGFR–EGF complexes back to the PM (Kornilova *et al.*, 1996; Kil *et al.*, 1999). Thus, perhaps a syntaxin 8-dependent mechanism might also be involved in the retrieval of EGF–EGFR complexes from the tubular REs back to the LE (Figure 11).

A role of syntaxin 8 in trafficking from EEs to LEs is supported by the effect of anti-syntaxin 8 antibody on EGFR trafficking in SLO-permeabilized HeLa cells. In agreement with the immunolocalization data, the anti-syntaxin 8 antibody diminished the early steps of EGFR transport from EEs. Note, however, that we never achieved >55% inhibition of EGFR degradation. The partial inhibition may indicate that at steady state syntaxin 8 is in complexes that are not accessible to the antibodies. The antibodies used for the EGFR trafficking assay have been raised against the H3 domain of syntaxin 8. Although this domain is critical for the syntaxin 8 function, the high stability of SNARE complexes might make it difficult for the antibody to compete with syntaxin 8 binding partners during the formation of a fusion complex. Alternatively, it is possible that the trafficking of EGFR is not synchronized in our system, and therefore some EGFR may have already reached the LE at the time we added the blocking antibody. Indeed, although the 18°C block does accumulate EGF in EEs, the block is not complete; thus it is likely that some of the endocytosed EGF had already traveled to the lysosomes by the time the anti-syntaxin 8 antibody was added to the permeabilized cells.

The ever-increasing understanding of the function of endosomal SNAREs is now allowing us to more fully define the different pathways of endosomal and lysosomal trafficking. Nevertheless, although we have begun to unravel the SNARE-dependent protein sorting and trafficking pathways, further investigation will be needed to fully understand the complexity of membrane trafficking and fusion pathways. In particular, little is known about the mechanism of SNARE localization or how a particular SNARE is matched to specific cargo. Furthermore, the specificity of vesicular trafficking is likely to emerge from a series of events that are mechanistically not yet clearly understood.

ACKNOWLEDGMENTS

We acknowledge Martin Steegmaier for the insightful discussions and technical help. We also thank Dr. Susan L. Palmieri (Stanford University, Cell Imaging facility) for assistance with confocal microscopy and Kelly C. Lee for technical assistance and critical reading of the manuscript. Tom van Rijn and Rene Scriwaneck are acknowledged for preparation of the electronmicrographs, and Elly van Donselaar is acknowledged for performing BSA-gold uptake in CHO cells. We also thank Suzie J. Scales for the critical reading of the manuscript.

REFERENCES

Advani, R.J., Bae, H.R., Bock, J.B., Chao, D.S., Doung, Y.C., Prekeris, R., Yoo, J.S., and Scheller, R.H. (1998). Seven novel mammalian SNARE proteins localize to distinct membrane compartments. J. Biol. Chem. *273*, 10317–10324.

Advani, R.J., Yang, B., Prekeris, R., Lee, K.C., Klumperman, J., and Scheller, R.H. (1999). VAMP-7 mediates vesicular transport from endosomes to lysosomes. J Cell Biol. *146*, 765–775.

Becherer, K.A., Rieder, S.E., Emr, S.D., and Jones, E.W. (1996). Novel syntaxin homologue, Pep12p, required for the sorting of lumenal hydrolases to the lysosome-like vacuole in yeast. Mol Biol Cell *7*, 579–594.

Bennett, M.K., Garcia-Arraras, J.E., Elferink, L.A., Peterson, K., Fleming, A.M., Hazuka, C.D., and Scheller, R.H. (1993). The syntaxin family of vesicular transport receptors. Cell *74*, 863–873.

Bennett, M.K., and Scheller, R.H. (1993). The molecular machinery for secretion is conserved from yeast to neurons. Proc. Natl. Acad. Sci. USA *90*, 2559–2563.

Bock, J.B., Klumperman, J., Davanger, S., and Scheller, R.H. (1997). Syntaxin 6 functions in trans-Golgi network vesicle trafficking. Mol. Biol. Cell *8*, 1261–1271.

Bock, J.B., and Scheller, R.H. (1997). A fusion of a new ideas. Nature *387*, 133–135.

Chao, D.S., Hay, J.C., Winnick, S., Prekeris, R., Klumperman, J., and Scheller, R.H. (1999). SNARE membrane trafficking dynamics in vivo. The J. Cell Biol. *144*, 869–881.

Fasshauer, D., Antonin, W., Margittai, M., Pabst, S., and Jahn, R. (1999). Mixed and noncognate SNARE complexes. J. Biol. Chem. *274*, 15440–15446.

Futter, C.E., Pearse, A., Hewlett, L.J., and Hopkins, C.R. (1996). Multivesicular endosomes containing internalized EGF-EGF receptor complexes mature and then fuse directly with lysosomes. J. Cell Biol. *132*, 1011–1023.

Galli, T., Chilcote, T., Mundigl, O., Binz, T., Niemann, H., and de Camilli, P. (1994). Tetanus toxin-mediated cleavage of cellubrevin impairs exocytosis of transferrin receptor-containing vesicles in CHO cells. J. Cell Biol. *125*, 1015–1024.

Geuze, H.J. (1998). The role of endosomes and lysosomes in MHC class II functioning. Immunol. Today *19*.

Gruenberg, J., Griffiths, G., and Howell, K.E. (1989). Characterization of the early endosome and putative endocytic carrier vesicles in vivo and with an assay of vesicle fusion in vitro. J. Cell Biol. *108*, 1301–1316.

Gruenberg, J., and Maxfield, F.R. (1995). Membrane transport in the endocytic pathway. Curr. Opin. Cell Biol. *7*, 552–563.

Hanson, P.I., Roth, R., Morisaki, H., Jahn, R., and Heuser, J.E. (1997). Structure and conformational changes in NSF and its membrane receptor complexes visualized by quick-freeze/deep-etch electron microscopy. Cell *90*, 523–535.

Hay, J.C., Hirling, H., and Scheller, R.H. (1996). Mammalian vesicle trafficking proteins of the endoplasmic reticulum and Golgi apparatus. J. Biol. Chem. *271*, 5671–5679.

Helenius, A., Mellman, I., Wall, D., and Hubbart, A. (1983). Endosomes. Trends Biochem. Sci. *8*, 245–250.

Holthuis, S.J., Nichols, B.J., Dhruvakumar, S., and Pelham, H.R. (1998a). Two syntaxin homologues in the TGN/endosomal system of yeast. EMBO J. *17*, 113–126.

Holthuis, J.C.M., Nichols, B.J., and Pelham, H.R.B. (1998b). The syntaxin Tlg1p mediates trafficking of chitin synthase III to polarized growth sites in yeast. Mol. Biol. Cell *9*, 3383–3397.

Hopkins, C.R. (1983). Intracellular routing of transferrin receptors in epidermoid carcinoma A431 cells. Cell *35*, 321–330.

Hopkins, C.R., and Trowbridge, I.S. (1983). Internalization and processing of transferrin and transferrin receptor in human carcinoma A431 cells. J. Cell Biol. *97*, 508–521.

Kil, S.J., Hobert, M., and Carlin, C. (1999). A leucine-based determinant in the epidermal growth factor receptor juxtamembrane domain is required for the efficient transport of ligand-receptor complexes to lysosomes. J. Biol. Chem. *274*, 3141–3150.

Klumperman, J., Kuliawat, R., Griffith, J.M., Geuze, H.J., and Arvan, P. (1998). Mannose-6-phosphate receptors are sorted from immature secretory granules via adaptor protein AP-1, clathrin, and syntaxin 6-positive vesicles. J. Cell Biol. *141*, 359–371.

Kornfield, S., and Mellman, I. (1989). The biogenesis of lysosomes. Annu. Rev. Cell Biol. *5*, 483–525.

Kornilova, E., Sorkina, T., Beguinot, L., and Sorkin, A. (1996). Lysosomal targeting of epidermal growth factor receptors via a kinase-dependent pathway is mediated by the receptor carboxy-terminal residues 1022–1123. J. Biol. Chem. *271*, 30340–30346.

Lin, R.C., and Scheller, R.H. (1997). Structural organization of the synaptic exocytosis core complex. Neuron *19*, 1087–1094.

Lippincott-Schwartz, J., Yuan, L.C., Tipper, C., Amherdt, M., Orci, L., and Klausner, R. (1991). Brefeldin A's effects on endosomes, lysosomes, and the TGN suggest a general mechanism for regulating organelle structure and membrane traffic. Cell *67*, 601–616.

Marsh, E.W., Leopold, P.L., Jones, N.L., and Maxfield, F.R. (1995). Oligomerized transferrin receptors are selectively retained by a lumenal sorting signal in a long-lived endocytic recycling compartment. J. Cell Biol. *129*, 1509–1522.

Mayor, S., Presley, J.F., and Maxfield, F.R. (1993). Sorting of membrane components from endosomes and subsequent recycling to the cell surface occurs by a bulk flow. J. Cell Biol. *121*, 1257–1269.

McMahon, H.T., Ushkaryov, Y.A., Edelmann, L., Link, E., Binz, T., Niemann, H., Jahn, R., and Sudhoff, T.C. (1993). Cellulobrevin is a ubiquitous tetanus-toxin substrate homologous to a putative synaptic vesicle fusion protein. Nature *364*, 346–349.

Mellman, I. (1996). Endocytosis and molecular sorting. Annu. Rev. Cell Dev. Biol. *12*, 575–625.

Prekeris, R., Klumperman, J., Chen, Y.A., and Scheller, R.H. (1998). Syntaxin 13 mediates cycling of plasma membrane proteins via tubulovesicular recycling endosomes. J. Cell Biol. *143*, 957–971.

Renfrew, C.A., and Hubbard, A.L. (1991). Sequential processing of epidermal growth factor in early and late endosomes in rat liver. J. Biol. Chem. *266*, 4348–4356.

Robinson, M.S., and Kreis, T.E. (1992). Recruitment of coat proteins onto Golgi membranes in intact and permeabilized cells: effect of brefeldin A and G protein activators. Cell *69*, 129–138.

Schmid, S.L. (1988). Two distinct subpopulations of endosomes involved in membrane recycling and transport to lysosomes. Cell *52*, 73–83.

Sheff, D.R., Daro, E.A., Hull, M., and Mellman, I. (1999). The receptor recycling pathway contains two distinct populations of early endosomes with different sorting functions. J. Cell Biol. *145*, 123–139.

Slot, J.W., Geuze, H.J., Gigengack, S., Lienhard, G.E., and James, D.E. (1991). Immuno-localization of the insulin regulatable glucose transporter in brown adipose tissue of the rat. J. Cell Biol. *113*, 123–135.

Slot, J.W., Geuze, H.J., and Weerkamp, A.H. (1988). Localization of Macromolecular components by application of the immunogold technique on cryosectioned bacteria. Methods Microbiol. *20*, 211–236.

Sollner, T., Bennett, M.K., Whiteheart, S.W., Scheller, R.H., and Rothman, J.E. (1993a). A protein assembly-disassembly pathway in vitro that may correspond to sequential steps of synaptic vesicle docking, activation, and fusion. Cell *75*, 409–418.

Sollner, T., Whiteheart, S.W., Brunner, M., Erdjument-Bromage, H., Geromanos, S., Tempst, P., and Rothman, J.E. (1993b). SNAP recep-

tors implicated in vesicle targeting and fusion [see comments]. Nature *362*, 318–324.

Steegmaier, M., Klumperman, J., Foletti, D.L., Yoo, J.S., and Scheller, R.H. (1999). VAMP4 is implicated in trans-Golgi network vesicle trafficking. Mol. Biol. Cell (*in press*).

Steegmaier, M., Yang, B., Yoo, J.S., Huang, B., Shen, M., Yu, S., Luo, Y., and Scheller, R.H. (1998). Three novel proteins in syntaxin/SNAP-25 family. J. Biol. Chem. *273*, 34171–34179.

Stoorvogel, W., Strous, G.J., Geuze, H.J., Oorschot, V., and Schwartz, A.L. (1991). Late endosomes derive from early endosomes by maturation. Cell *65*, 417–427.

Sutton, R.B., Fasshauer, D., Jahn, R., and Brunger, A.T. (1998). Crystal structure of a SNARE complex involved in synaptic exocytosis at 2, 4A resolution. Nature *395*, 347–353.

Wang, H., Frelin, L., and Pevsner, J. (1997). Human syntaxin 7: a Pep12p/Vps6p homologue implicated in vesicle trafficking to lysosomes. Gene *199*, 39–48.

Wong, S.H., Xu, Y., Zhang, T., and Hong, W. (1998a). Syntaxin 7, a novel syntaxin member associated with the early endosomal compartment. J. Biol. Chem. *273*, 375–380.

Wong, S.H., Zhang, T., Xu, Y., Subramaniam, N., Griffiths, G., and Hong, W. (1998b). Endobrevin, a novel synaptobrevin/VAMP-like protein preferentially associated with the early endosome. Mol. Biol. Cell *9*, 1549–1563.

Yamashiro, D., Tycko, B., Fluss, S., and Maxfield, F.R. (1984). Segregation of transferrin to a mildly acidic (pH 6.5) para-Golgi compartment in the recycling pathway. Cell *37*, 789–800.

Yang, B., Gonzalez, L., Prekeris, R., Steegmaier, M., Advani, R., and Scheller, R.H. (1999). SNARE interactions are not selective: implications for membrane fusion specificity. J. Biol. Chem. *274*, 5649–5653.

Zeng, Q., Subramaniam, V.N., Wong, S.H., Tang, B.L., Parton, R.G., Rea, S., James, D.E., and Hong, W. (1998). A novel synaptobrevin/VAMP homologous protein (VAMP5) is increased during in vitro myogenesis and present in the plasma membrane. Mol. Biol. Cell *9*, 2423–2437.